UPR proteins IRE1 and PERK switch BiP from chaperone to ER stress sensor

Megan C Kopp[1], **Natacha Larburu**[1], **Vinoth Durairaj**[1], **Christopher J Adams**[1], **Maruf MU Ali**[1,*]

[1]Department of Life Sciences, Sir Ernst Chain Building, Imperial College London, London SW7 2AZ, UK

Abstract

BiP is a major ER chaperone and suggested to act as primary sensor in the activation of the unfolded protein response (UPR). How BiP operates as a molecular chaperone and as an ER stress sensor is unknown. Here, by reconstituting components of human UPR, ER stress and BiP chaperone systems, we discover that the interaction of BiP with the luminal domains (LD) of UPR proteins, IRE1 and PERK, switch BiP from its chaperone cycle into an ER stress sensor cycle by preventing the binding of its cochaperones, with loss of ATPase stimulation. Furthermore, misfolded protein-dependent dissociation of BiP from IRE1 is primed by ATP but not ADP. Our data elucidate a previously unidentified mechanistic cycle of BiP function that explains its ability to act as a Hsp70 chaperone and ER stress sensor.

Introduction

The unfolded protein response (UPR) is a signaling system that detects misfolded proteins within the endoplasmic reticulum (ER) and coordinates a cellular response that aims to restore protein homeostasis. There are three key UPR signal activators, IRE1, PERK and ATF6 that give rise to separate branches of the response[1–4]. The activator proteins traverse the ER membrane presenting a luminal domain (LD) that is involved in signal detection; they also possess cytosolic effector domains that propagate the signal[3,4]. The LD of UPR

proteins participate in detecting misfolded protein leading to UPR activation. IRE1 LD and PERK LD share a high degree of structural similarity[5–7], suggesting that they operate the same mechanism for detecting misfolded proteins. The cytosolic portions of both IRE1 and PERK contain a kinase domain that auto-phosphorylates in trans[8–11]. Activated PERK then phosphorylates eIF2a, which ephemerally leads to global mRNA translation attenuation[11]. IRE1 phosphorylation results in stimulation of endoribonuclease activity which splices mRNA of XBP1 to form a potent transcriptional activator[12–16]. This acts to upregulate UPR target genes such as chaperones, which then help to alleviate the burden of misfolded proteins within the ER[1–3].

The chaperone, BiP, is one of the most abundant proteins within the ER[17]. It operates a typical Hsp70 chaperone-substrate mechanism that involves recruitment of misfolded proteins to BiP substrate-binding domain (SBD) by J-domain cochaperones[18–20]. This greatly stimulates ATPase activity within the nucleotide binding domain (NBD), enabling BiP to adopt an ADP-bound (low K_{on} and K_{off}) closed conformation which traps misfolded protein substrate. The exchange of ADP to ATP by nucleotide exchange factors (NEF) permits transition to an open conformation (high K_{on} and K_{off}) that releases the bound protein substrate[18,19].

Besides its role as a major ER chaperone, BiP has been suggested to be a direct ER stress sensor leading to UPR activation[4]. BiP binds to the UPR activator proteins, IRE1 and PERK via its NBD and it's release is dependent upon misfolded protein binding to BiP SBD[21,22]. This is possibly followed by binding of misfolded protein to LD to further enhance UPR activation[23] leading to IRE1 association with ribosomes which may affect ER protein folding load[24]. BiP may also bind to IRE1 via SBD to repress UPR signaling[25]. However, the precise mechanistic details of UPR signal activation are unclear.

The ability of BiP to function as an ER stress sensor[21,22], suggests that it acts independently of its well characterized Hsp70 chaperone-substrate regulated cycle in as yet an unknown method. To shed light on the mechanistic events that determine how BiP operates as a molecular chaperone and as an ER stress sensor, we reconstitute components of UPR, ER stress, and BiP chaperone complex systems and assess the relationship between them using biochemical methods to inform us of molecular mechanism. We discover a previously unknown BiP ER stress sensor cycle that explains its ability to operate both as a Hsp70 chaperone in complex with its cochaperone proteins and as a sensor of ER stress in the UPR.

Results

IRE1 and PERK inhibit BiP ATPase stimulation

The ATPase activity of a Hsp70 chaperone is an integral part of its chaperone mechanism[18,19]. To determine what effect IRE1 and PERK has upon BiP ATPase activity, we recombinantly expressed and purified components of human BiP chaperone complex system including its J-protein containing cochaperone, ERdj3, and NEF, Sil1, along with the LD of human UPR proteins, IRE1 and PERK. The ATPase activity was followed colorimetrically at 620 nm wavelength as a result of free orthophosphate binding to a molybdate moiety causing a colour change upon ATP hydrolysis (Fig. 1). BiP had a low

inherent ATPase activity (rate of Pi release = 0.080 pmol/μl/min) that was stimulated almost 5-fold on addition of ERdj3 and Sil1 (rate= 0.386 pmol/μl/min) (Fig. 1b and g, Supplementary Table 1). The characteristic stimulation of ATPase activity by J-protein and NEF was consistent with that of a typical Hsp70 type chaperone. When IRE1 LD and PERK LD were added to BiP without its cochaperones, there was no significant difference in the ATPase activity (Fig. 1c, g), with BiP retaining its low inherent ATPase level, indicating that IRE1 LD and PERK LD had no direct effect on BiP ATPase activity (Fig. 1 and Supplementary Table 1). Next, we assessed the ATPase activity when adding either individual or both cochaperones, ERdj3 and Sil1, together with IRE1 LD or PERK LD (Fig. 1d-g and Supplementary Table 1). We observed a reduction in BiP ATPase activity on addition of IRE1 LD and PERK LD to basal BiP levels in the presence of either single cochaperone or the whole chaperone complex encompassing both ERdj3 and Sil1 (Fig. 1d-g and Supplementary Table 1). This indicates that the addition of IRE1 LD and PERK LD caused loss of BiP ATPase stimulation by its J-domain cochaperone and NEF but retained its low inherent ATPase activity, which was unaffected by IRE1 LD and PERK LD.

Folded or misfolded IRE1 LD affect BiP ATPase activity differently

Thus far, the impact of UPR proteins and cochaperones on BiP ATPase activity were measured in the absence of misfolded protein. We repeated the BiP ATPase measurements, but added C_H1[21,26], an immunoglobulin fragment that is inherently misfolded in the absence of its binding partner C_L. The addition of C_H1 stimulated BiP ATPase activity. Stimulation by misfolded protein was further observed in each sample in which either or both Sil1 and ERdj3 cochaperones were added, at a higher level than without C_H1 (Fig. 2a,b and Supplementary Table 2). However, the addition of IRE1 LD had an inhibitory effect, with the ATPase rate showing a reduction compared to samples that lacked IRE1 LD. Thus, misfolded proteins stimulate BiP ATPase activity, whereas IRE1 LD has an inhibitory effect on BiP ATPase stimulation even in the presence of misfolded protein.

Misfolded proteins associate with BiP to form a chaperone substrate interaction via BiP SBD; in contrast, IRE1 LD binds to BiP NBD[21,22,27], although a UPR functional association that represses signaling has also been reported with SBD[25] (see discussion). The binding of both C_H1 and IRE1 LD to BiP are mutually exclusive[21]. We considered whether we could reverse the inhibitory effect of IRE1 LD by inducing its denaturing to mimic authentic misfolded protein, C_H1. In this scenario, IRE1 LD would possibly change the way it associates to BiP from interacting with NBD to SBD as a chaperone substrate upon denaturation. Exposure to elevated temperatures is a typical method to induce protein misfolding. We heated IRE1 LD to 55°C for 30 mins and then observed its elution profile by size exclusion chromatography and compared it to before heat treatment. IRE1 LD protein eluted, for the most part, as a dimer with small fraction forming a tetramer. However, heat treated IRE1 LD eluted exclusively in the void volume of the column indicating that the protein was aggregated and denatured as a result of thermal treatment (Fig. 2c).

To assess differences in binding between folded IRE1 LD and misfolded IRE1 LD to BiP, we measured their binding affinities to both wild type BiP (BiP^{WT}) and a BiP SBD mutant, V461F (BiP^{V461F}) [28,29], using microscale thermophoresis (MST). This mutation prevents

misfolded protein engagement to BiP SBD as a chaperone-substrate (Fig. 2d). Folded IRE1 LD interacted with both BiP^{WT} and BiP^{V461F} with similar affinity (Fig. 2e,f and Supplementary Table 3). This suggests that folded IRE1 LD does not interact with BiP via its SBD as a chaperone-substrate. By contrast, misfolded IRE1 LD interacted with BiP^{WT} but failed to associate with BiP^{V461F} (Fig. 2g,h and Supplementary Table 3), indicating that misfolded IRE1 LD binds to BiP SBD. Thus, folded and misfolded IRE1 LD act in contrasting fashion by binding to different domains of BiP.

We then assessed the impact of misfolded IRE1 LD on BiP ATPase activity in the presence of its cochaperones. Misfolded IRE1 LD stimulated BiP ATPase activity in the presence of either or both Sil1 and ERdj3 to similar levels observed with C_H1. This is the opposite effect seen with folded IRE1 LD, which had an inhibitory impact on BiP ATPase activity (Fig. 2i,j and Supplementary Table 4). Therefore, we were able to reverse the inhibitory effects of folded IRE1 LD on BiP ATPase stimulation by inducing its misfolding, which in turn, stimulated BiP ATPase activity similar to C_H1. This indicates differences in the way BiP functions when interacting with folded IRE1 LD and misfolded IRE1 LD, consistent with its dual role as a chaperone and an ER stress sensor.

Binding of UPR proteins and cochaperones to BiP is mutually exclusive

The observation that IRE1 LD and PERK LD inhibit stimulation of BiP ATPase, but not its inherent ATPase activity, suggests that IRE1 LD and PERK LD prevent the association of ERdj3 and Sil1 to BiP by competing for the same binding site on BiP NBD. To test this notion, we conducted a series of competitive pull-down assays, in which GST tagged BiP was incubated with either ERdj3 or Sil1 (Fig. 3a; Extended Data Fig. 1), and then increasing concentrations of IRE1 LD and PERK LD were added. The experiments indicate that when BiP formed a chaperone complex with ERdj3 or with Sil1, increasing concentrations of IRE1 LD (Fig. 3b,c) and PERK LD (Fig. 3d,e) outcompeted Sil1 and ERdj3 for binding to BiP. Thus, the data demonstrate that binding to BiP by UPR proteins and BiP cochaperones are mutually exclusive.

To identify a mutation that affects LD association with BiP and to obtain further evidence that LD and Sil1 have overlapping binding sites on BiP, we examined the crystal structure of yeast BiP NBD in complex with Sil1[30] (Fig. 3f). At the interface, a Lysine residue (Lys314) of BiP mediates a number of polar contacts with Sil1[30]; moreover, this residue and surrounding ones are well conserved across all BiP species. We reasoned that mutation of that Lys to a bulky Phe would deleteriously impact binding, by disrupting the polar interactions at the interface and by sterically blocking association with binding partner(s). We mutated the equivalent Lys residue in human BiP (Lys294) in GST tagged BiP (BiP^{K294F}) (Extended Data Fig. 2 and 3) and assessed binding to cochaperones and UPR proteins by pull-down assay and MST analysis. The pull-down assays suggested that BiP^{K294F} disrupted the interaction between BiP and its cochaperones, Sil1 and ERdj3; but more importantly, it inhibited the binding of IRE1 LD and PERK LD to BiP (Fig. 3g). Analysis of binding affinities by MST suggested a loss of specific binding between BiP^{K294F} and IRE1 LD or PERK LD (Fig. 3h,i and Supplementary Table 5). The binding profiles did indicate small fluctuations in fluorescence, but the data did not fit a binding saturation curve.

For Sil1, there was a considerable reduction in strength of binding to BiP[K294F] (Figure 3j and Supplementary Table 5). Similarly, ERdj3 also displayed a reduced affinity for BiP[K294F] although the reduction in binding strength was less than that observed for Sil1 (Fig. 3k and Supplementary Table 5). This suggests that the interaction between BiP NBD and its cochaperones, particularly ERdj3, may involve other contact sites. Indeed, ERdj3 possesses a J-domain, which is known to bind to a pocket between the NBD and the SBD of Hsp70s, contacting the interdomain linker[31].

Thus, we identify a mutation in BiP that inhibits binding to IRE1 LD and PERK LD. The mutation reinforces the evidence that the interaction site for IRE1 LD and PERK LD is in the NBD of BiP, consistent with other studies[21,22,27]. BiP cochaperones also interact with this site but may have other substantial contacts with BiP[31]. The mutational analyses, along with the competitive pull-down experiments, suggest that BiP interaction with UPR proteins and cochaperones are mutually exclusive. By inhibiting the binding of cochaperones to BiP, the UPR proteins prevent BiP from functioning effectively as a chaperone; however, BiP still retains its ability to bind and detect misfolded proteins via its SBD.

Effect of nucleotides on BiP interactions

We have previously demonstrated that the interaction between LD and BiP is independent of nucleotides[21,22]. To support those previous observations, we measured the interaction between IRE1 LD and PERK LD to BiP in the presence of ATP and ADP using MST and extended our measurements to analyze the influence of nucleotides on BiP interaction with its cochaperones. The binding affinities for BiP interaction with IRE1 LD and PERK LD in the absence and in the presence of nucleotides were similar (Fig. 3h,i; Fig. 4a,b and Supplementary Table 6), indicating that association between BiP and LD is largely unaffected by nucleotides. The interaction between BiP and its cochaperones, ERdj3 and Sil1, increased in strength on addition of nucleotides when compared to BiP (Fig. 3j,k; Fig 4c,d and Supplementary Table 6). These results show that binding between LD and BiP is not influenced by nucleotides.

Given that the interaction between BiP NBD and IRE1 LD is independent of nucleotide influence, the dissociation of BiP from IRE1 LD would be solely dependent upon misfolded protein binding to BiP SBD. We considered whether nucleotides could sensitize or prime BiP SBD to detect misfolded proteins, whilst bound to IRE1 LD, thereby facilitating its release. To determine the effect of nucleotides on the ability of BiP to detect misfolded proteins whilst in complex with IRE1 LD, we used our in vitro FRET based assay[22,32]. This assay measures an interaction between IRE1 LD and BiP NBD via N-terminally tagged FRET CFP and YFP fluorophores (Fig. 5a). The binding of misfolded proteins to BiP SBD induces a conformational change that mediates BiP dissociation from IRE1 LD with corresponding loss of FRET signal from which we can deduce the IC_{50} value and the inhibition constant (K_i).

We first assessed whether ADP, ATP or AMP-PNP, a non-hydrolysable analogue of ATP, caused any dissociation of YFP-BiP and CFP-IRE1 LD complex by measuring loss of FRET signal. Consistent with our MST experiments (Fig. 4) and our previous in vitro protein interaction analysis[21,22], we found that addition of nucleotides at all concentrations tested

did not cause any loss in the FRET signal, indicating that there was no dissociation of BiP-IRE1 LD complex (Fig. 5b, 5c and 5d and Extended Data Fig. 4). However, upon addition of C_H1 we observed complete loss of FRET signal, thus demonstrating that dissociation of BiP-IRE1 LD complex is dependent upon misfolded protein association. Next, we incubated CFP-IRE1 LD and YFP-BiP in the absence and in the presence of either ATP, ADP, AMP-PNP, and then measured the FRET signal on addition of varying concentration of misfolded protein, C_H1. The inhibition profile of FRET signal displayed a two-phase response for all samples tested including APO, ATP, AMP-PNP and ADP (Fig. 5e-h and Supplementary Table 7). The inhibition constant for the low concentration phase (Ki^{low}) were similar for both ADP and ATP but differed for AMP-PNP and greatly differed for APO state. The inhibition constant for the high concentration phase (Ki^{High}) is a more significant measurement than the Ki^{low}, as this is the concentration required for full dissociation of FRET complex (YFP-BiP and CFP-IRE1 LD). Interestingly, the Ki^{High} for FRET complex incubated with ADP ($Ki^{High} = 4.3 \pm 0.4\mu M$) was similar to APO FRET complex ($Ki^{High} = 5.2 \pm 0.6\mu M$) but significantly greater for the FRET complex when enriched with ATP ($Ki^{High} = 0.2 \pm 0.01\mu M$). The Ki^{High} for FRET complex when bound to AMP-PNP ($Ki^{High} = 0.6 \pm 0.05\mu M$) was similar to addition of ATP, consistent with AMP-PNP being an ATP mimic. The ATP bound BiP-IRE1 LD complex requires 21-fold less C_H1 to inhibit the FRET signal and facilitate dissociation than the ADP bound FRET complex. The addition of ATP increases the sensitivity of BiP-IRE1 LD complex for C_H1, whereas ADP abrogates the sensitivity and priming effect. Thus, ATP – but not ADP – primes IRE1-BiP SBD to sense misfolded protein, the binding of which facilitates BiP dissociation via NBD from UPR proteins.

Discussion

In the current study, we reconstitute components of UPR, ER stress, and BiP chaperone complex systems and assess their relationships. We identify a previously unknown ER stress sensor cycle (Fig. 6) that explains how BiP functions as a Hsp70 chaperone and as an ER stress sensor.

The binding of UPR proteins inhibit BiP ATPase stimulation by preventing the association of cochaperones. The inhibitory effect of UPR proteins can be reversed by denaturing IRE1 LD, resulting in BiP stimulation similar to C_H1. Our data suggest that BiP can interact with IRE1 in one of two ways. Firstly, as a UPR signaling partner protein that binds via NBD and inhibits BiP ATPase stimulation. Secondly, as a chaperone that binds via BiP SBD that stimulates BiP ATPase activity. We have previously reported that IRE1 LD interacts with BiP NBD, using a combination of techniques including: pull-down assays, MST, chemical cross-linking[21], and in vitro FRET measurements[22]. This interaction has also been observed in another study using genetic analysis[27]. Furthermore, overexpression of NBD was shown to reduce IRE1 phosphorylation in cells[21]. Here, we utilized the Sil1-BiP crystal structure to identify a mutation within the NBD that inhibits binding between LD and BiP.

The inhibition of ATPase stimulation by IRE1 prevents BiP from functioning effectively as a Hsp70 type chaperone. In this bound state, however, BiP still retains the ability to engage misfolded proteins and act as a stress sensor. These two modes of binding and action

highlight the different roles that BiP plays, both as an ER stress sensor and a Hsp70 chaperone. It is the association of UPR proteins that causes BiP to switch from its chaperone role to that of an ER stress sensor.

The interaction between BiP NBD and IRE1 LD is independent of nucleotides. The dissociation of the complex is solely dependent on misfolded protein binding to BiP SBD. However, nucleotides do influence the ability of BiP SBD to engage misfolded proteins. BiP that is bound to IRE1 LD has a greater sensitivity towards misfolded protein in the presence of ATP. In contrast, the priming of BiP to sense misfolded proteins is reversed or desensitized when BiP is bound to ADP, with over 21-fold increase in misfolded protein concentration required to facilitate the same level of dissociation as the ATP bound BiP-IRE1 LD complex on addition of C_H1.

Interestingly, the dissociation of BiP from IRE1 occurs in two phases comprising of a low and high concentration phase irrespective of whether BiP is bound with various nucleotides or not. Although we do not know what these phases are, we speculate that the first phase could be a breakdown in oligomer species to form a single heterodimer complex, with the second phase being the dissociation of heterodimer. Alternatively, it may represent two distinct conformations of BiP that are required to enable full dissociation.

The discriminatory effects of different nucleotides on BiP ability to engage misfolded protein whilst bound to IRE1, is analogous to protein translocation across the inner mitochondrial membrane, where mitochondrial Hsp70 bound to a component of the inner membrane translocon, Tim44, engages the emerging translocating polypeptide chain in an ATP primed state[33] but not ADP bound form.

In the primed state, IRE1 and PERK prevent the association of BiP cochaperones and nucleotide exchange factors to ensure that ATP turnover and exchange is halted so that BiP is geared towards sensing misfolded proteins. Once BiP that is bound to IRE1, engages misfolded protein via its SBD, it engenders an allosteric change that alters its affinity for IRE1 causing its releases – a process that is suggested to be coupled to UPR activation[21,34]. This enables BiP to interact with its cochaperones again and revert to its chaperone cycle with misfolded substrate in tow.

Our results also suggest a possible explanation for observations that indicate ATP triggers the dissociation of BiP-IRE1 co-immune complexes from cell lysates[34]. Present within the cell lysate are numerous peptides and proteins that have exposed hydrophobic patches and are partially misfolded. The addition of ATP would prime BiP SBD to engage misfolded protein without affecting IRE1-BiP NBD interaction, leading to enhanced misfolded protein dependent dissociation of the complex.

Analysis of binding affinities indicate that in the absence of ER stress, IRE1 will be bound with BiP. This association favours BiP acting as a stress sensor. In this state, BiP is unable to conduct its normal chaperone function as it cannot bind to its cochaperones. IRE1 is a scarce protein with 500—5000 copies in HeLa cells[35]. By contrast, BiP is one of the most abundant proteins in the ER with estimates suggesting around 2×10^7 as a baseline number[17]. Assuming all cellular IRE1 is occupied with BiP in the absence of UPR, it would have

minimal effect on the total number of free BiP that could participate in protein folding and chaperone activity.

BiP detects its client substrate protein to activate UPR in a ratiometric fashion[17]. BiP that is bound to IRE1 would bind misfolded protein via its SBD and compete with chaperone productive free BiP to engage its client proteins. The huge difference in concentration between BiP that is bound to IRE1 and chaperone productive BiP, would protect against UPR activation at low misfolded protein levels, but would facilitate a graded response, with saturation of chaperone productive BiP, along with IRE1 bound BiP, leading to full UPR activation. In our model, IRE1 does not participate in competition with misfolded protein for association to BiP, as its interaction to BiP is mediated via NBD[4].

After UPR activation and a reduction in misfolded protein levels, the vast disparity in concentration between free BiP and IRE1, would favour an equilibrium that drives BiP to re-associate with IRE1 leading to UPR repression. The inhibited state with BiP bound to IRE1 would represent the default ground state, in agreement with their cellular concentrations[17,35] and binding affinity analysis.

Besides our model in which BiP acts as an ER stress sensor, there are two further established models that seek to explain how UPR activation occurs. An alternative BiP dependent model suggests that BiP interacts with IRE1 via SBD to inhibit UPR signaling analogous to heat shock factor 1 repression by Hsp70[36]. There is also a direct association model that demonstrates binding of misfolded protein to IRE1 LD to activate UPR[23]. One speculative scenario that can reconcile certain aspects of the different models suggest that upon ER stress, BiP detects misfolded protein via its SBD leading to reduced affinity of BiP NBD for IRE1 and subsequent dissociation. This triggers IRE1 dimerization and low level UPR signaling. The departure of BiP reveals a binding site on IRE1 (MHC-like peptide groove) that can now engage misfolded protein resulting in oligomerization and full scale UPR activation. To remove the bound misfolded protein from the peptide groove, BiP could re-associate with IRE1 but this time via its SBD - in cooperation with J-protein - to capture the misfolded protein from IRE1. However, exactly how these different mechanisms are interconnected is not clear and further work is required to understand this process in better detail.

In summary, the binding of IRE1 and PERK switch BiP into stress sensor cycle where ATP primes BiP to engage misfolded proteins, thereby facilitating dissociation of complex. Our study rationalizes how BiP can act as the major ER Hsp70 chaperone and as a primary detector of ER stress.

Methods

Expression and Purification

Human BiP (28-654), IRE1 LD (32-440), PERK LD (105-403) proteins were cloned and expressed with a N-terminal His$_6$- tag or a N-terminal GST-tag followed by a PreScission Protease cleavage site. Human ERdj3 (23-358aa) and yeast Sil1 (20-421aa) were cloned into pGEX 6p1 vector containing a GST-tag and PreScission protease site. Fluorescent fusion

constructs were designed with fluorescent proteins, CFP and YFP, attached N-terminally to human IRE1 LD and BiP via a short 15aa linker (GGAGGAGGAGGAGGA) (Kopp *et al.* 2018)[22] that were cloned into pGEX 6p1 vector. All constructs were expressed in *Escherichia coli* BL21 (DE3) cells (Agilent, CA), and were grown in autoinduction medium with trace elements (Formedia, UK) at 37°C for 3 hrs and then overnight at 22°C with the exception of ERdj3 which was grown for 1 hr at 37°C then overnight at 18°C. His$_6$-tag proteins were purified by Co^{2+}-NTA affinity using TALON metal affinity resin (Clontech, CA,) in buffer A (50 mM HEPES pH 8.0, 400 mM NaCl) and eluted in the presence of 250 mM imidazole. GST-tagged proteins were purified using Agarose Glutathione Affinity resin (ThermoFisher, MA). GST- proteins were bound to resin and washed three times in buffer B (50 mM HEPES pH 7.3, 400 mM NaCl, 1 mM DTT), and once in a high salt buffer containing 1M NaCl. Proteins were eluted with buffer C (50 mM HEPES pH 8.0, 400 mM NaCl,1mM DTT, 10mM reduced glutathione). Cell lysis (sonication) and the initial BiP purification step were supplemented with 5 mM ATP and 10 mM MgCl$_2$. The His$_6$-tag or GST-tag were removed by overnight incubation with PreScission Protease at 4°C followed by an additional affinity purification step to remove uncleaved protein. All proteins were further purified by anion-exchange using a HiTrap Q HP column (GE Healthcare, UK) and size-exclusion chromatography on a HiLoad 16/60 Superdex 200 column in buffer D (50 mM HEPES pH 8.0, 200 mM NaCl, 1 mM DTT). For experiments, proteins were diluted into buffer E (50 mM HEPES pH 8.0, 50 mM NaCl, 10 mM MgCl$_2$, 10 mM KCl). The misfolded protein C$_H$1 was expressed and purified following the previously described protocol (Feige *et al* 2009)[26]. For thermal treatment of IRE1 LD, protein samples were kept at 55°C for 30 mins and then passed through a Superdex 200 10/300 Increase size-exclusion column. Estimation of multimeric states and void volume were based on comparison with known protein standards.

ATPase Assay

The Malachite Green Phosphate Kit solutions were used for experiments (Abnova, TW). A standard curve created from a serial dilution of K$_2$PO$_4$ was used to determine phosphate concentrations during experiments. Reaction samples were prepared for each 5-minute time point measured between 0-120 minutes. BiP at 5 μM concentration was used in all experiments, to which 5 μM of each component (IRE1 LD, PERK LD, ERdj3, or Sil1) were added in various combinations, making sure that stimulatory proteins (ERdj3 and Sil1) were in equimolar concentration with inhibitory proteins (IRE1 LD or PERK LD). The reaction mixtures were incubated with 1 mM ATP at room temperature (RT) for the specified time point, after which samples were quenched with 12 μL of the acid solution and left at RT for 10 min, then 34 μL of the Malachite Green solution was added to each sample and incubated for 20 min, according to manufactures protocol. Samples were then transferred to a 384 well microplate (Greiner Bio-one, AT) and absorbance was measured at 620 nM wavelength on a CLARIOstar® microplate reader (BMG Labtech, DE).

Microscale Thermophoresis

MST experiments were performed using a Monolith NT.115 instrument (Nanotemper Technologies, DE). BiP^{WT}, BiP^{V461F} and BiP^{K294F} were labelled using the Monolith NT Protein Labelling Kit Red-NHS. Then, ~100 nM labelled BiP was mixed with 1 mM

nucleotide where indicated and incubated on ice for 30 min in MST buffer (50 mM HEPES pH 7.8, 50 mM NaCl, 10 mM KCl, 10 mM MgCl$_2$, 0.1% TWEEN-20). This mixture was then combined with equal volumes of a sixteen two-fold serial dilution of the unlabeled binding partner. Experiments were carried out in hydrophobic treated capillaries with 20% LED power and 80% IR-laser at 25 °C. Data were analyzed on Graphpad Prism 8 (Graphpad Software, CA, USA) and K$_d$ was determined using one site binding saturation curve fit.

Single Mutant and Competition Pull-down assay

All pull-down experiments were conducted in 2 mL gravity flow columns. Glutathione resin pre-equilibrated with buffer E was incubated with 40 μM of the GST-tagged BiP^{WT} or BiP^{K294F} for 1 hr at RT. The resin was washed with 500 μL of buffer E to remove the unbound BiP. Then 50 μL of 120 μM IRE1, PERK, ERdj3, or Sil1 as indicated was added to the column and incubated for 1 hr at RT. The resin was washed with 500 μL of buffer E in 125 μL increments and resuspended in 75 μL of buffer E. Samples of the re-suspended resin were analyzed on a 4-12% gradient SDS-PAGE gel.

For the competition pull-downs, 75 μL of Glutathione resin pre-equilibrated with buffer E was incubated with 20 μM GST tagged BiP (GST-BiP). The resin was washed with 500 μL of buffer E to remove the unbound BiP. Then 50 μL of 60 μM ERdj3 or Sil1 was added to each column and incubated for 1 hr at RT. The resin was then washed with 500 μL of buffer E in 125 μL increments. IRE1 LD or PERK LD was added to each column at increasing concentrations (0 μM, 15 μM, 30 μM, 60 μM, 75 μM, 90 μM, and 120 μM) and incubated for 1 hr at RT. Resin was washed again as mentioned earlier and re-suspended with 75 μL of buffer E. Samples of the re-suspended resin were analyzed on a 4-12% gradient SDS-PAGE gel.

FRET Assay

FRET assay experiments were carried out using a CLARIOstar® microplate reader (BMG Labtech, DE) following the protocol for measuring a three-way protein-protein interaction using FRET from Martin *et al* (2008)[32] and Kopp *et al* (2018)[22] for apo protein. In brief, a mixture containing 30 μM of each fluorescent protein (CFP-IRE1 LD and YFP-BiP), and increasing concentrations of C$_H$1 were made into a volume of 160 μL in buffer E. Next, 50 μL was transferred to a 384 well microplate (Greiner Bio-one, AT). The protocol was adapted for nucleotide experiments to include a 30 min incubation at RT with 1mM nucleotide in the reaction mixture. Calculation of Ki was based on the protocol from Martin *et al* (2008)[32]. The data were plotted using percentage inhibition as a function of the C$_H$1 concentration and fitted to an exponential curve (two phase association), from which 50% dissociation value or IC$_{50}$ (equivalent to half-life) for each phase were measured in GraphPad prism 8. These values were then used to calculate the Ki for each phase.

## Statistics and reproducibility

Sample sizes and statistical tests where applicable for experiments are denoted in the figure legends. Analysis and graphs were generated in GraphPad prism 8 and excel.

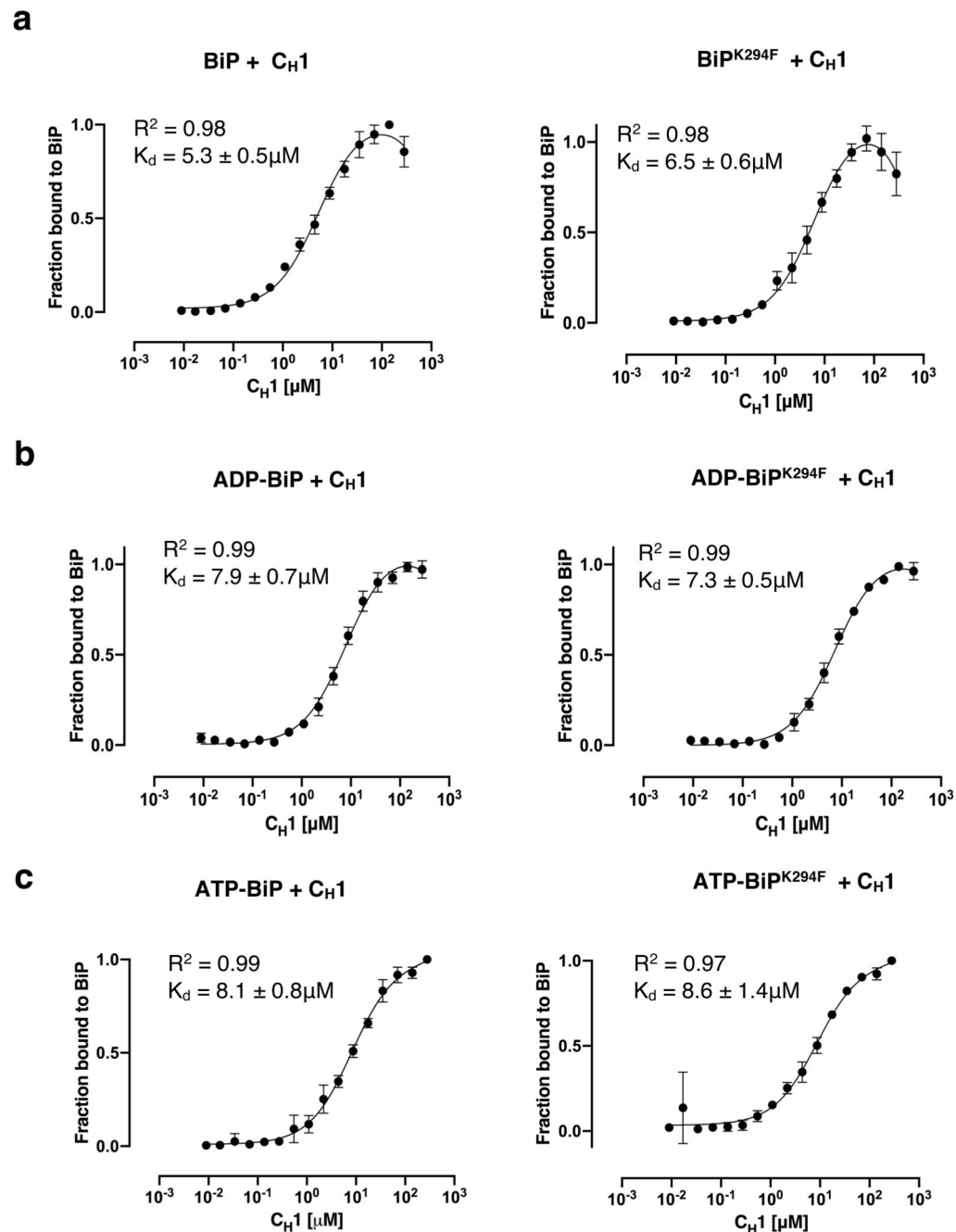**Extended Data**

a

b

c
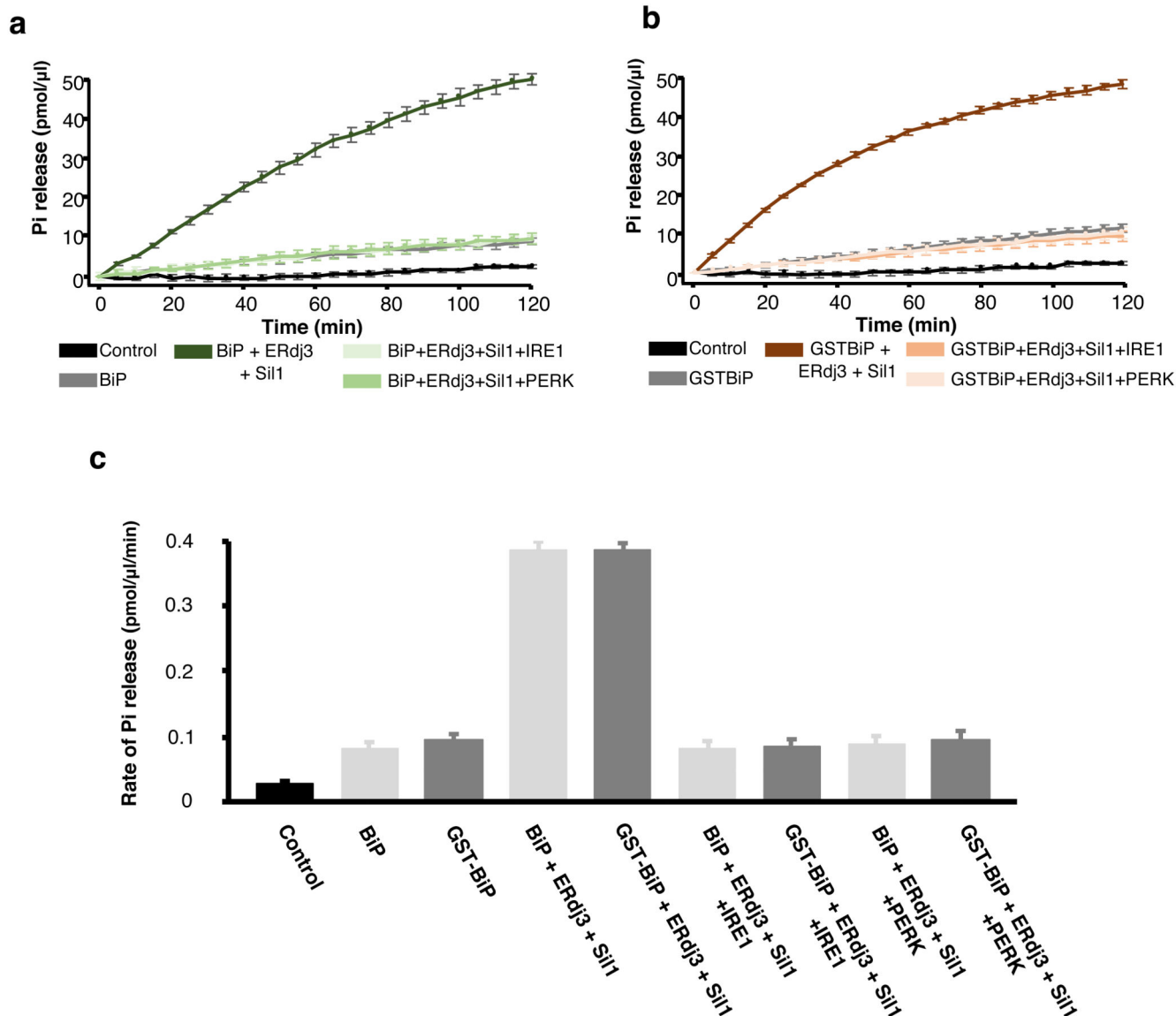
Extended Data Fig. 1. Comparison of BiP and GST-BiP stimulation and inhibition.
(a) BiP ATPase activity showing stimulation by co-chaperones and inhibition by IRE1 and PERK LD. (b) same as (a), but using GST tagged BiP. (c) A comparison of the rate of ATPase activity for BiP and GST tagged BiP. Both tagged and untagged BiP are stimulated by co-chaperones and inhibited by IRE1 and PERK LD to the same level, indicating that the attachment of GST to BiP had no effect on BiP ATPase stimulation or inhibition. Statistics as in Figure 1, source data available online.
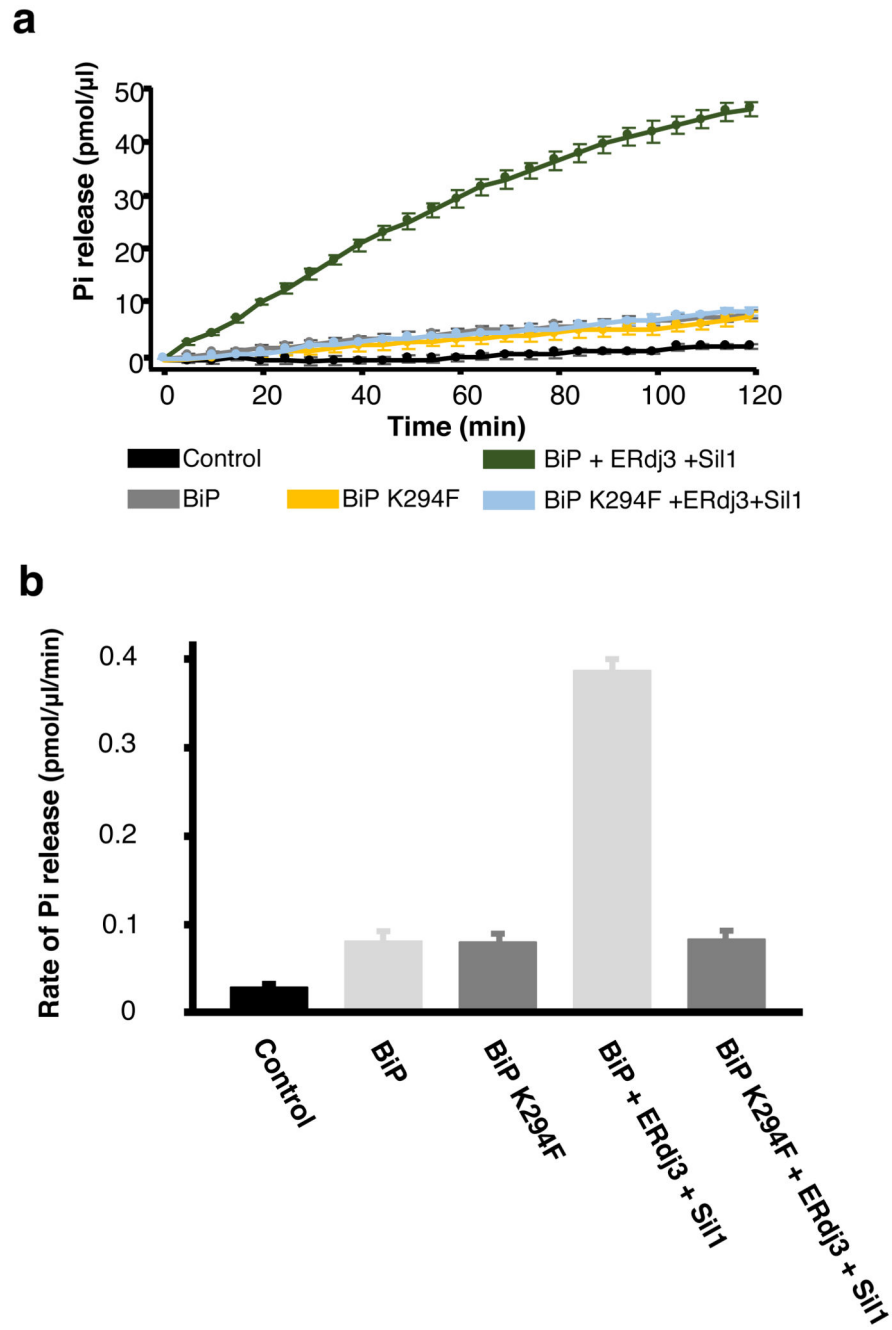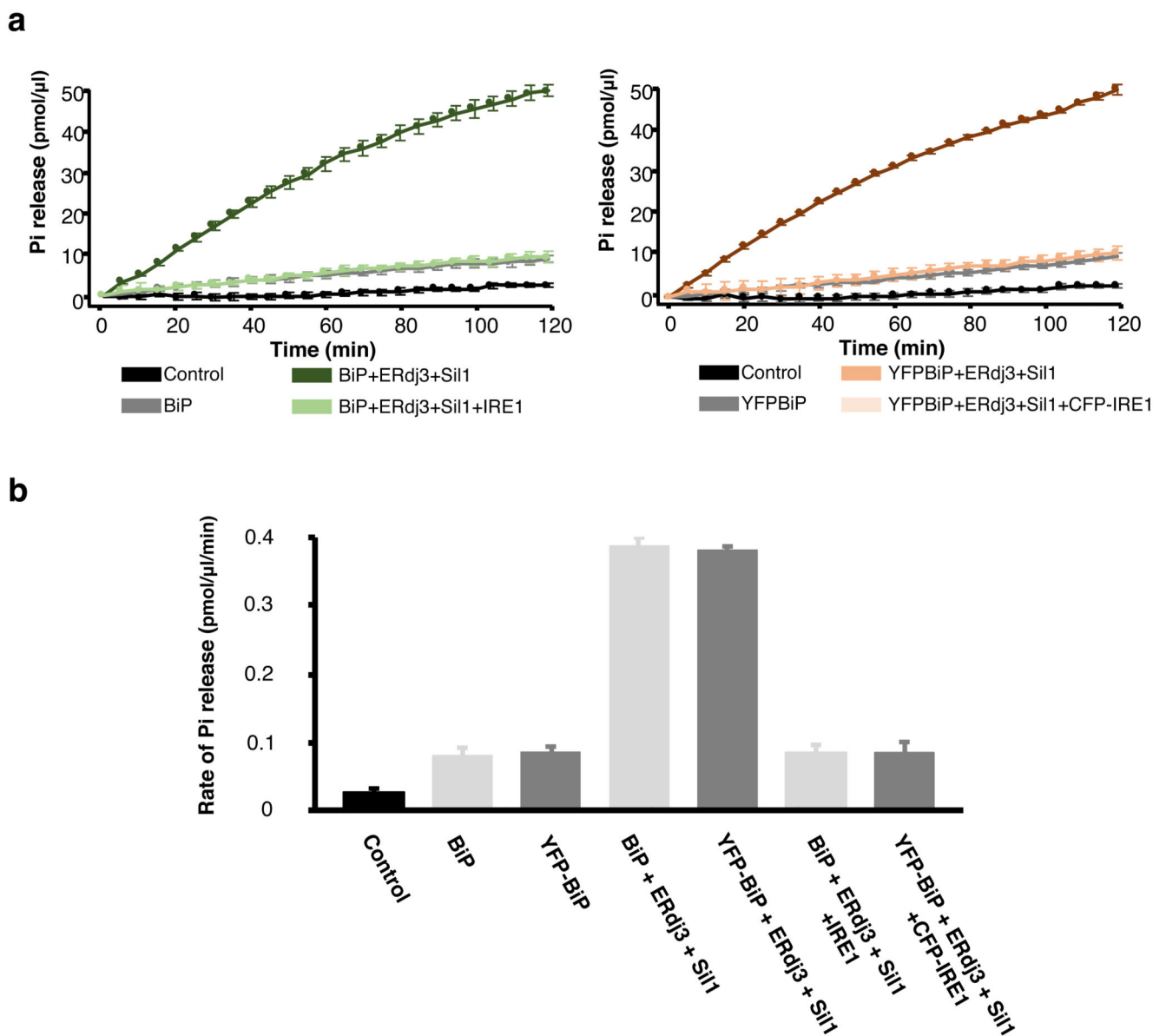
Extended Data Fig. 2. Mutant BiP^{K294F} has same basal ATPase activity as BiP^{WT}.
(a) BiP^{K294F} ATPase activity on addition of co-chaperones. (b) A comparison of the rate of ATPase activity for BiP and BiP^{K294F}. The K294F mutation based within the BiP NBD, had no effect on inherent BiP ATPase, but prevents ATPase stimulation consistent with-it inhibiting co-chaperone binding. Statistics as in Figure 1, source data available online.

a

b

c

Extended Data Fig. 3. Assessment of BiP^{K294F} affinity for C$_H$1 in presence of nucleotides.
BiP^{K294F} has same binding affinity for C$_H$1, in different nucleotide bound states, as BiP^{WT}.
(a) MST profile measuring the binding affinity between BiP and BiP^{K294F} for C$_H$1. (b) same
as (a), but in the presence of ADP. (C) same as (a), but with ATP. The experiments indicate
that the mutation had no effect on BiP interaction with misfolded substrate protein or
affected BiP nucleotide bound conformations. Statistics as in Figure 4, source data available
online.

a

b

Extended Data Fig. 4. Attachment of YFP had no effect on BiP functionality

(a) ATPase activity of BiP and YFP tagged BiP. (b) Comparison of the rate of ATPase activity for BiP and YFP- tagged BiP on addition of co-chaperones and CFP-IRE1 LD. The attachment of YFP had no effect on BiP basal activity, or stimulation by co-chaperones, or inhibition by CFP tagged IRE1 LD. Statistics as in Figure 1, source data available online.

Supplementary Material

Refer to Web version on PubMed Central for supplementary material.

Acknowledgements

References

1. Hetz C, Papa FR. The Unfolded Protein Response and Cell Fate Control. Mol Cell. 2017

2. Wang M, Kaufman RJ. Protein misfolding in the endoplasmic reticulum as a conduit to human disease. Nature. 2016; 529:326–335. [PubMed: 26791723]

3. Walter P, Ron D. The unfolded protein response: from stress pathway to homeostatic regulation. Science. 2011; 334:1081–1086. [PubMed: 22116877]

4. Adams CJ, Kopp MC, Larburu N, Nowak PR, Ali MMU. Structure and Molecular Mechanism of ER Stress Signaling by the Unfolded Protein Response Signal Activator IRE1. Front Mol Biosci. 2019; 6:11. [PubMed: 30931312]

5. Zhou J, et al. The crystal structure of human IRE1 luminal domain reveals a conserved dimerization interface required for activation of the unfolded protein response. Proc Natl Acad Sci USA. 2006; 103:14343–14348. [PubMed: 16973740]

6. Credle JJ, Finer-Moore JS, Papa FR, Stroud RM, Walter P. On the mechanism of sensing unfolded protein in the endoplasmic reticulum. Proc Natl Acad Sci USA. 2005; 102:18773–18784. [PubMed: 16365312]

7. Carrara M, Prischi F, Nowak PR, Ali MMU. Crystal structures reveal transient PERK luminal domain tetramerization in endoplasmic reticulum stress signaling. EMBO J. 2015; 34:1589–1600. [PubMed: 25925385]

8. Shamu CE, Walter P. Oligomerization and phosphorylation of the Ire1p kinase during intracellular signaling from the endoplasmic reticulum to the nucleus. EMBO J. 1996; 15:3028–3039. [PubMed: 8670804]

9. Tirasophon W, Welihinda AA, Kaufman RJ. A stress response pathway from the endoplasmic reticulum to the nucleus requires a novel bifunctional protein kinase/endoribonuclease (Ire1p) in mammalian cells. Genes Dev. 1998; 12:1812–1824. [PubMed: 9637683]

10. Ali MMU, et al. Structure of the Ire1 autophosphorylation complex and implications for the unfolded protein response. EMBO J. 2011; 30:894–905. [PubMed: 21317875]

11. Harding HP, Zhang Y, Ron D. Protein translation and folding are coupled by an endoplasmic-reticulum-resident kinase. Nature. 1999; 397:271–4. [PubMed: 9930704]

12. Shamu CE, Walter P. Oligomerization and phosphorylation of the Ire1p kinase during intracellular signaling from the endoplasmic reticulum to the nucleus. EMBO J. 1996; 15:3028–3039. [PubMed: 8670804]

13. Tirasophon W, Welihinda AA, Kaufman RJ. A stress response pathway from the endoplasmic reticulum to the nucleus requires a novel bifunctional protein kinase/endoribonuclease (Ire1p) in mammalian cells. Genes Dev. 1998; 12:1812–1824. [PubMed: 9637683]

14. Cox JS, Walter P. A novel mechanism for regulating activity of a transcription factor that controls the unfolded protein response. Cell. 1996; 87:391–404. [PubMed: 8898193]

15. Calfon M, et al. IRE1 couples endoplasmic reticulum load to secretory capacity by processing the XBP-1 mRNA. Nature. 2002; 415:92–6. [PubMed: 11780124]

16. Prischi F, Nowak PR, Carrara M, Ali MMU. Phosphoregulation of Ire1 RNase splicing activity. Nat Commun. 2014; 5

17. Bakunts A, et al. Ratiometric sensing of BiP-client versus BiP levels by the unfolded protein response determines its signaling amplitude. Elife. 2017; 6

18. Hartl FU, Bracher A, Hayer-Hartl M. Molecular chaperones in protein folding and proteostasis. Nature. 2011; 475:324–332. [PubMed: 21776078]

19. Kampinga HH, Craig EA. The HSP70 chaperone machinery: J proteins as drivers of functional specificity. Nat Rev Mol Cell Biol. 2010; 11:579–92. [PubMed: 20651708]

20. Behnke J, Feige MJ, Hendershot LM. BiP and its nucleotide exchange factors Grp170 and Sil1: mechanisms of action and biological functions. J Mol Biol. 2015; 427:1589–1608. [PubMed: 25698114]

21. Carrara M, Prischi F, Nowak PR, Kopp MC, Ali MMU. Noncanonical binding of BiP ATPase domain to Ire1 and Perk is dissociated by unfolded protein CH1 to initiate ER stress signaling. Elife. 2015; 4

22. Kopp MC, Nowak PR, Larburu N, Adams CJ, Ali MMU. In vitro FRET analysis of IRE1 and BiP association and dissociation upon endoplasmic reticulum stress. Elife. 2018; 7

23. Karagoz GE, Acosta-Alvear D, Walter P. The Unfolded Protein Response: Detecting and Responding to Fluctuations in the Protein-Folding Capacity of the Endoplasmic Reticulum. Cold Spring Harb Perspect Biol. 2019

24. Acosta-Alvear D, et al. The unfolded protein response and endoplasmic reticulum protein targeting machineries converge on the stress sensor IRE1. Elife. 2018; 7

25. Amin-Wetzel N, et al. A J-Protein Co-chaperone Recruits BiP to Monomerize IRE1 and Repress the Unfolded Protein Response. Cell. 2017; 171:1625–1637.e13. [PubMed: 29198525]

26. Feige MJ, et al. An unfolded CH1 domain controls the assembly and secretion of IgG antibodies. Mol Cell. 2009; 34:569–579. [PubMed: 19524537]

27. Todd-Corlett A, Jones E, Seghers C, Gething M-J. Lobe IB of the ATPase domain of Kar2p/BiP interacts with Ire1p to negatively regulate the unfolded protein response in Saccharomyces cerevisiae. J Mol Biol. 2007; 367:770–787. [PubMed: 17276461]

28. Petrova K, Oyadomari S, Hendershot LM, Ron D. Regulated association of misfolded endoplasmic reticulum lumenal proteins with P58/DNAJc3. EMBO J. 2008; 27:2862–2872. [PubMed: 18923430]

29. Laufen T, et al. Mechanism of regulation of hsp70 chaperones by DnaJ cochaperones. Proc Natl Acad Sci USA. 1999; 96:5452–5457. [PubMed: 10318904]

30. Yan M, Li J, Sha B. Structural analysis of the Sil1-Bip complex reveals the mechanism for Sil1 to function as a nucleotide-exchange factor. Biochem J. 2011; 438:447–455. [PubMed: 21675960]

31. Kityk R, Kopp J, Mayer MP. Molecular Mechanism of J-Domain-Triggered ATP Hydrolysis by Hsp70 Chaperones. Mol Cell. 2018; 69:227–237 e4. [PubMed: 29290615]

32. Martin, SF, Tatham, MH, Hay, RT, Samuel, IDW. Protein Sci. Vol. 17. Cold Spring Harbor Laboratory Press; 2008. Quantitative analysis of multi-protein interactions using FRET: application to the SUMO pathway; 777–784.

33. Craig EA. Hsp70 at the membrane: driving protein translocation. BMC Biol. 2018; 16:11. [PubMed: 29343244]

34. Bertolotti A, Zhang Y, Hendershot LM, Harding HP, Ron D. Dynamic interaction of BiP and ER stress transducers in the unfolded-protein response. Nat Cell Biol. 2000; 2:326–332. [PubMed: 10854322]

35. Boisvert FM, et al. A quantitative spatial proteomics analysis of proteome turnover in human cells. Mol Cell Proteomics. 2012; 11

36. Preissler S, Ron D. Early Events in the Endoplasmic Reticulum Unfolded Protein Response. Cold Spring Harb Perspect Biol. 2018
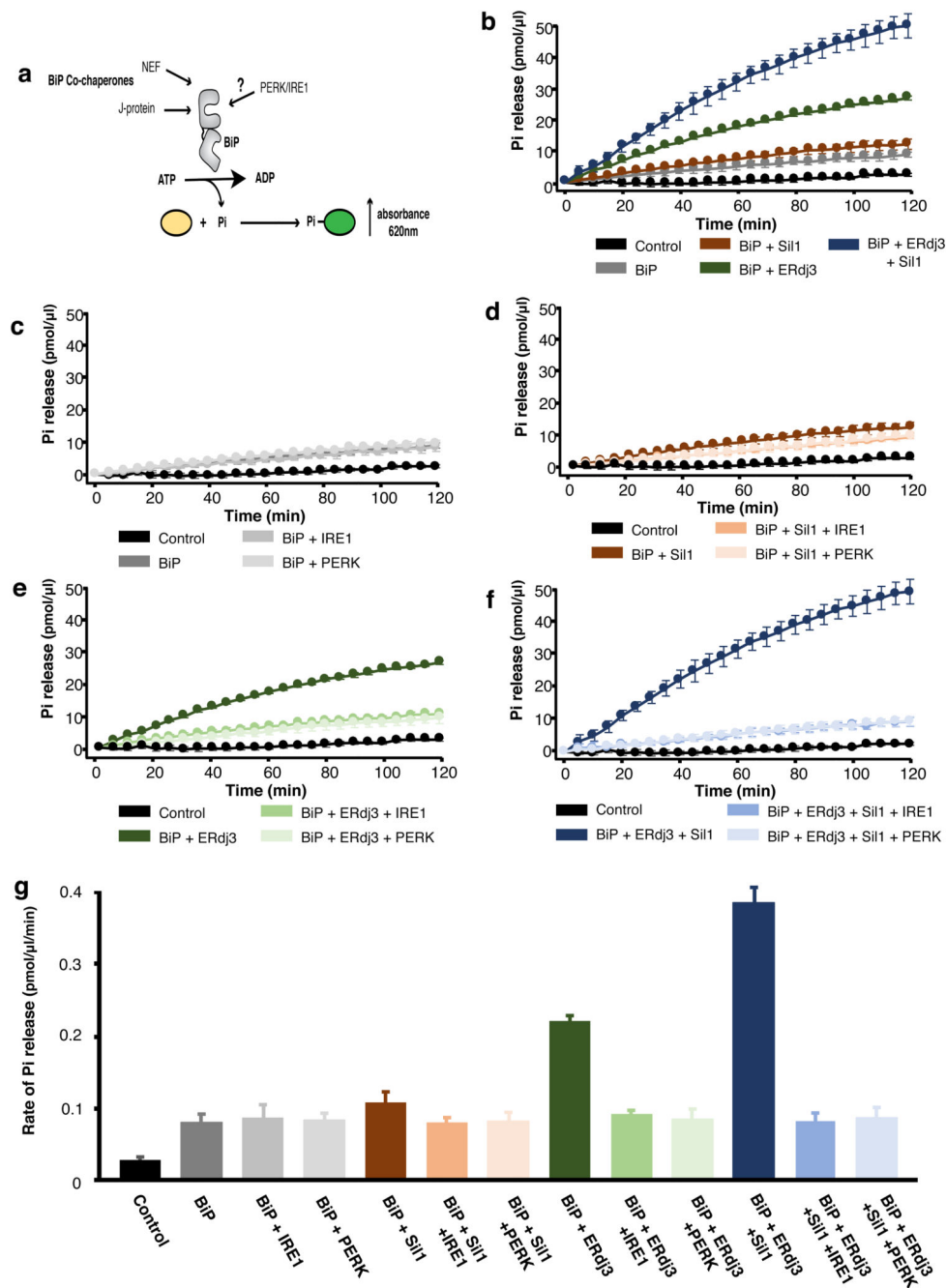
Figure 1. IRE1 and PERK LD cause loss of BiP ATPase stimulation by cochaperone and NEF effectors, but BiP retains its inherent activity.

a, Schematic representation of assay used for measuring ATPase activity. **b-f**, Graphs displaying phosphate (Pi) release over time as a result of BiP ATPase activity. Data shown are mean ± sd, from nine independent experiments. Source data available online. BiP displayed low basal ATPase activity; the addition of Sil1 slightly increased activity, whereas ERdj3 or both cochaperone Sil1 and ERdj3 together greatly stimulated BiP activity (**b**). Addition of IRE1 LD or PERK LD did not affect BiP basal ATPase activity (**c**) but reversed

the stimulation by Sil1 (**d**), by ERdj3 (**e**), and by both cochaperones ERdj3 and Sil1 together (**f**). **g**, Bar graph showing the rates of BiP ATPase activity upon addition of effector proteins. Data are mean ± sd, from nine independent experiments. ATPase rates are in Supplementary Table 1.
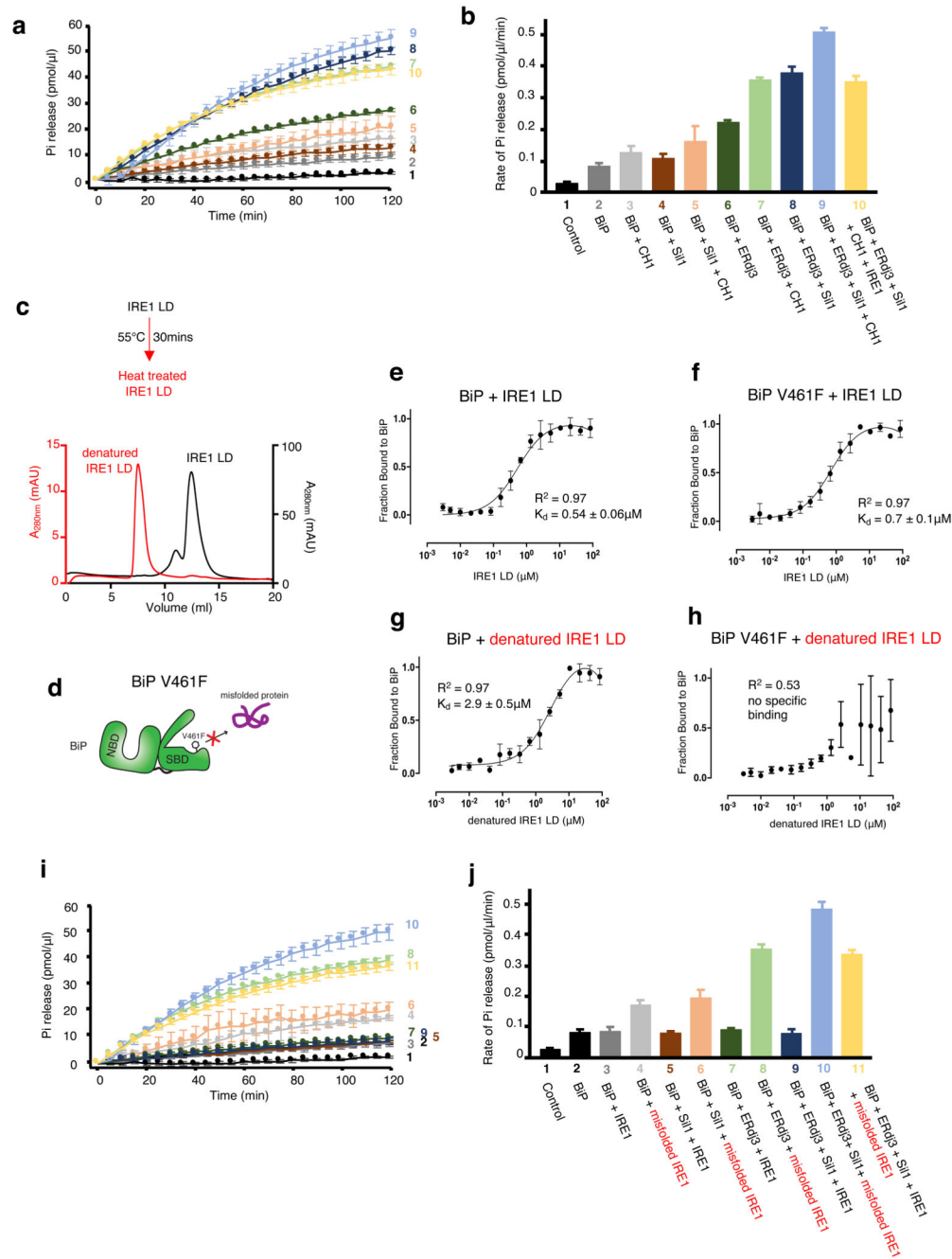
Figure 2. Folded and misfolded IRE1 LD have different effects on BiP interaction and activity.
a-b, ATPase assay that measured BiP activity on addition of C_H1 misfolded protein with cochaperones and IRE1 LD. Pi release over time (**a**) and rate of BiP ATPase activity (**b**) deduced from **a**. Data are mean ± sd from nine independent experiments. **c**, Size exclusion chromatography of IRE1 LD heat treated (55°C for 30 mins, red) or untreated control (black). The heat-treated sample eluted in the void volume indicating protein aggregation. **d**, A graphical representation of BiP V461F mutant. The SBD mutant prevents the engagement of misfolded chaperone-substrate protein to BiP[28,29]. **e-f**, Microscale thermophoresis (MST)

profile of folded IRE1 LD interaction with BiP^{WT} (**e**) or BiP^{V461F}(**f**). The binding affinities are comparable and suggest folded IRE1 LD does not engage the SBD as a chaperone substrate. **g-h**, MST profile of misfolded IRE1 LD interaction with BiP^{WT} (**g**), and BiP^{V461F}(**h**). Data points in **e-h** are mean ± sd from three independent experiments. **i,** BiP ATPase assay comparing the effects of folded and misfolded IRE1 on BiP activity in the presence of cochaperones. **j**, rate of BiP ATP activity deduced from **i** (mean ± sd, n=9 independent experiments). Source data for graphs are available online. ATPase rate values for **b** and **j** are listed in Supplementary Tables 2 and 4. Binding affinities are in Supplementary Table 3.
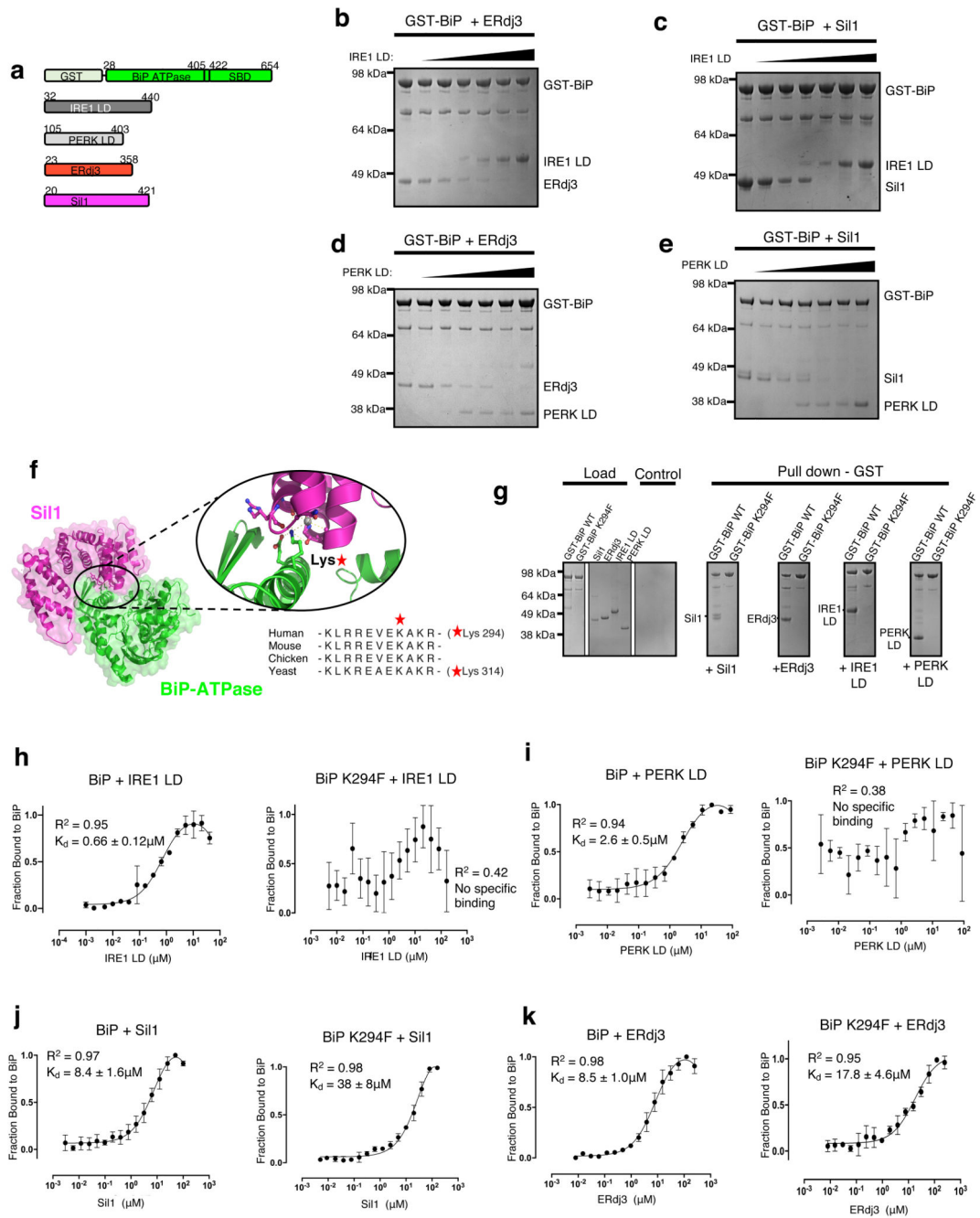
Figure 3. UPR proteins and cochaperones have mutually exclusive binding sites on BiP NBD that are impacted by BiP^K294F mutant.

a, Schematic representation of the various constructs used for the pull-down assay, with the numbers denoting the residue number of the protein. **b**, Competitive pull-down assay in which increasing concentrations of IRE1 LD were added to GST-BiP – ERdj3 chaperone complex. IRE1 LD outcompeted ERdj3 for binding to BiP, suggesting mutually exclusive binding. **c**, Competitive pull-down assay where GST-BiP - Sil1 complex was immobilized to beads and increasing concentrations of IRE1 LD were added. **d**, Same as (**b**), but with PERK

LD. **e**, Same as (**c**), but with PERK LD. **f**, Crystal structure of BiP ATPase – Sil1 complex (PDB 3QML), highlighting the interface between interacting molecules. BiP NBD domain residue Lys314 (corresponding to Lys294 in human) mediates key polar contacts between the two molecules. Sequence alignment (right) indicated that this residue is highly conserved across BiP species. **g**, Pull-down assay to assess interaction of GST- BiP^{WT} or BiP^{K294F} mutant with cochaperones and UPR proteins IRE1 LD and PERK LD. **h-k**, MST experiments comparing the binding affinity of GST tagged BiP^{WT} and BiP^{K294F} to cochaperones and UPR proteins. Data are mean ± sd from 3 independent experiments. Source Data are available online. BiP^{K294F} mutant disrupted binding to IRE1 LD (**h**) and PERK LD (**i**). The BiP^{K294F} mutant displayed greatly reduced binding affinity for Sil1 compared to BiP^{WT} (**j**). The BiP^{K294F} mutant displayed reduced, but still substantial binding for ERdj3 indicating that ERdj3 may have other contact sites with BiP. Uncropped gel images are available as Source Data. Binding affinities are in Supplementary Table 5.
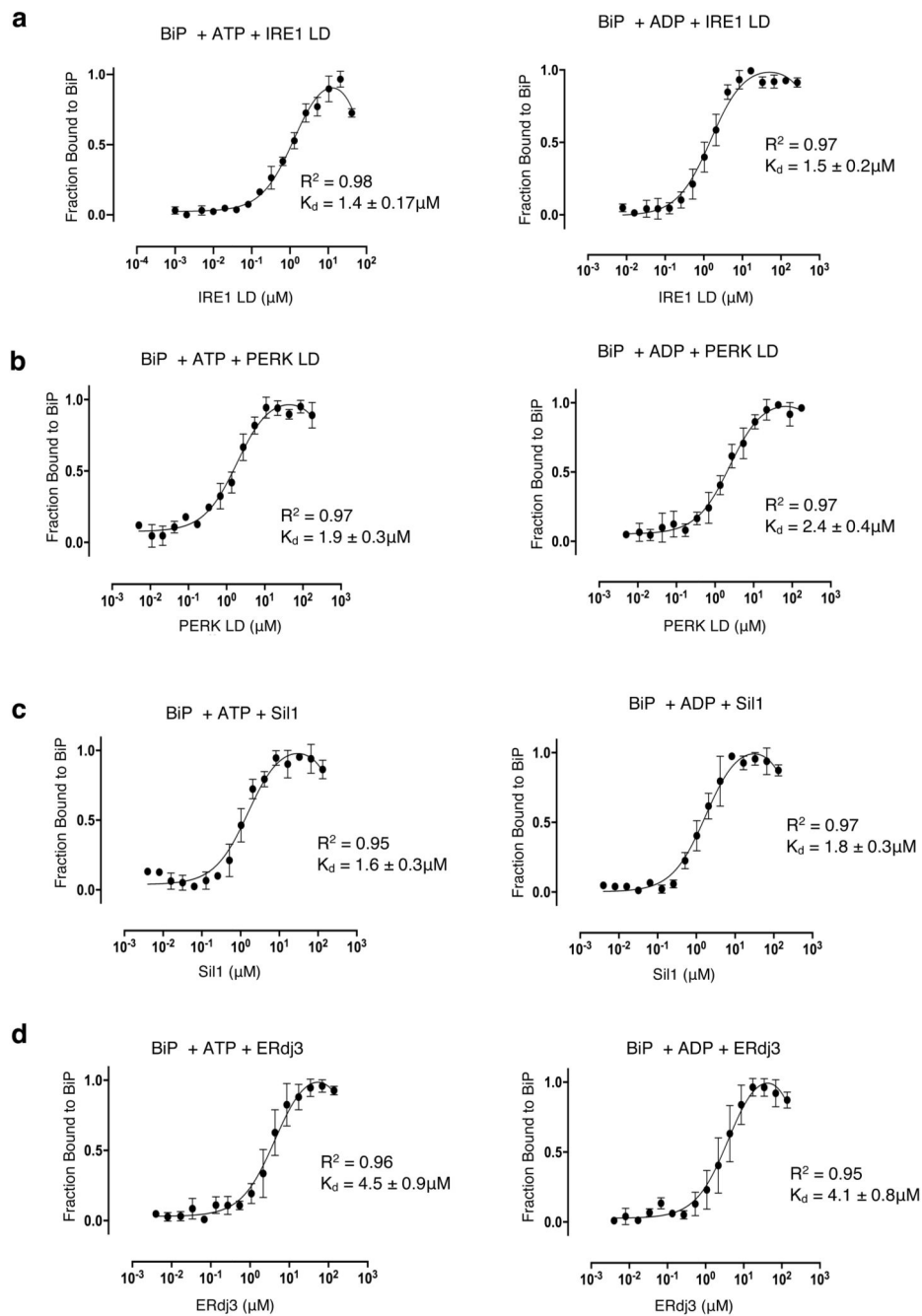
Figure 4. The effect of nucleotides on BiP binding to UPR proteins and cochaperones.
MST profiles measuring the binding between GST tagged BiP with UPR proteins and with cochaperones in the presence of ATP and ADP. **a,** The binding affinities for BiP association to IRE1 LD in the presence of ATP and ADP are similar to the binding affinity without nucleotides (Figure 3h). **b,** PERK LD incubated with ATP and ADP are similar to the binding affinity without nucleotides (Figure 3i). **c-d,** Sil1 (**c**) and ERdj3 (**d**) both show stronger binding to BiP with nucleotide present than without nucleotides (Figure 3 j-k). Data

are mean ± sd from 3 independent experiments. Source Data are available online. Binding affinities are in Supplementary Table 6.
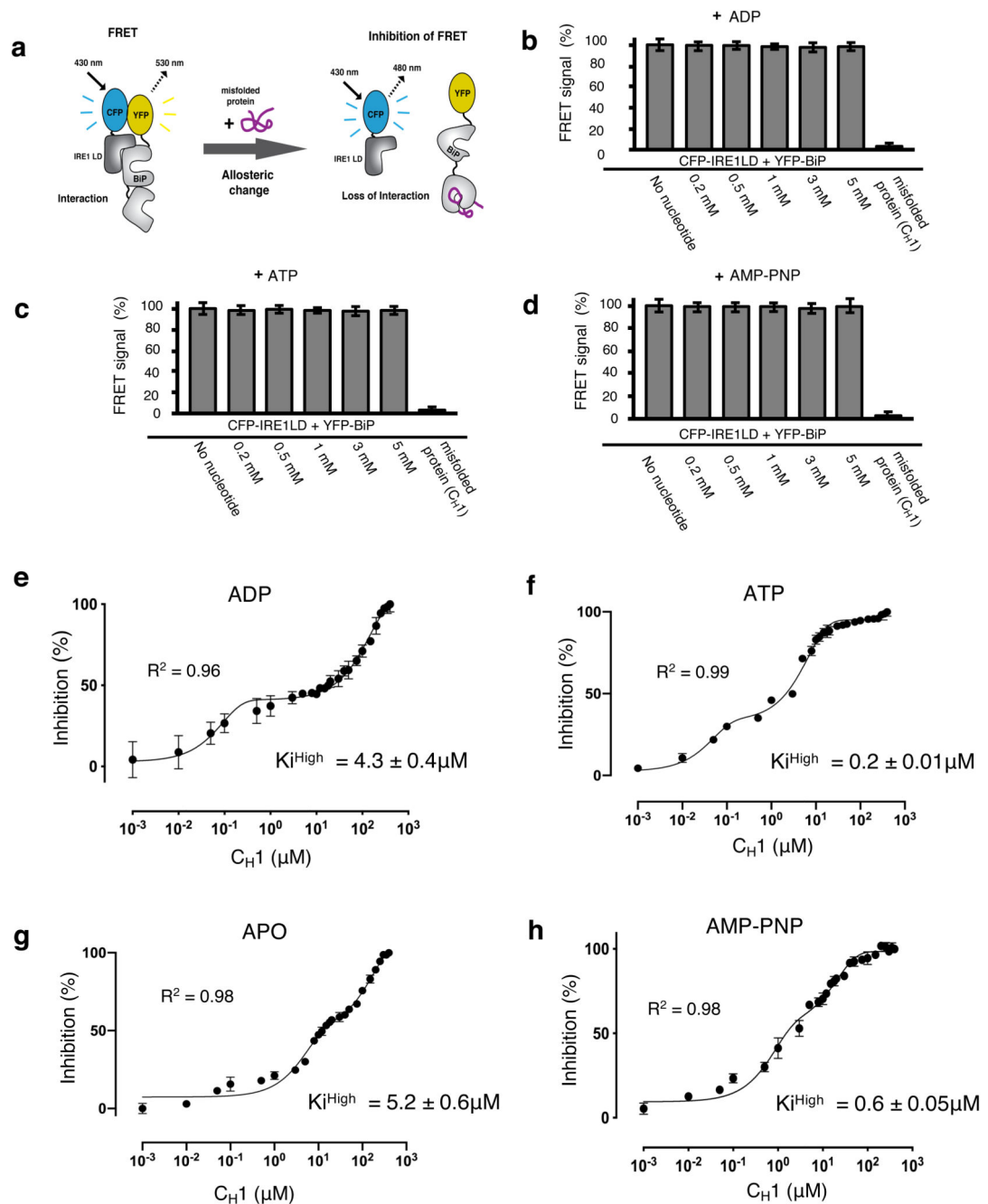
Figure 5. ATP – but not ADP – primes and facilitates the release of BiP from IRE1 LD.
a, Experimental design for three-component in vitro UPR FRET assay[22,32] used to measure the inhibition of CFP-IRE1 – YFP-BiP complex by misfolded protein in the presence and absence of nucleotides. **b-d**, Bar graph showing FRET signal observed upon addition of ADP (**b**), ATP (**c**) or AMP-PNP (**d**). In each case, FRET inhibition due to dissociation of the complex was solely dependent on binding of misfolded protein C_H1. Data are mean ± s.d., n=9 independent experiments. **e-h,** FRET signal inhibition (%) as a function of the C_H1 concentration in the absence and presence of different nucleotides: ADP (**e**), ATP (**f**), APO

(**g**) and AMP-PNP (**h**). Data were fitted to exponential curve (two phase association) and the IC_{50} (equivalent to half-life) for each phase was deduced. The IC_{50} measurement was then used to calculate the Ki[32]. The ATP bound BiP-IRE1 LD complex required 21-fold less misfolded protein to facilitate full dissociation of complex than the ADP bound state, suggesting a priming effect towards misfolded protein on ATP addition. Data are mean ± s.d., n = 9 independent experiments. Source Data are available online. The IC_{50} and inhibition constant values for both low and high concentration phases in the absence and presence of different nucleotides are in Supplementary Table 7.
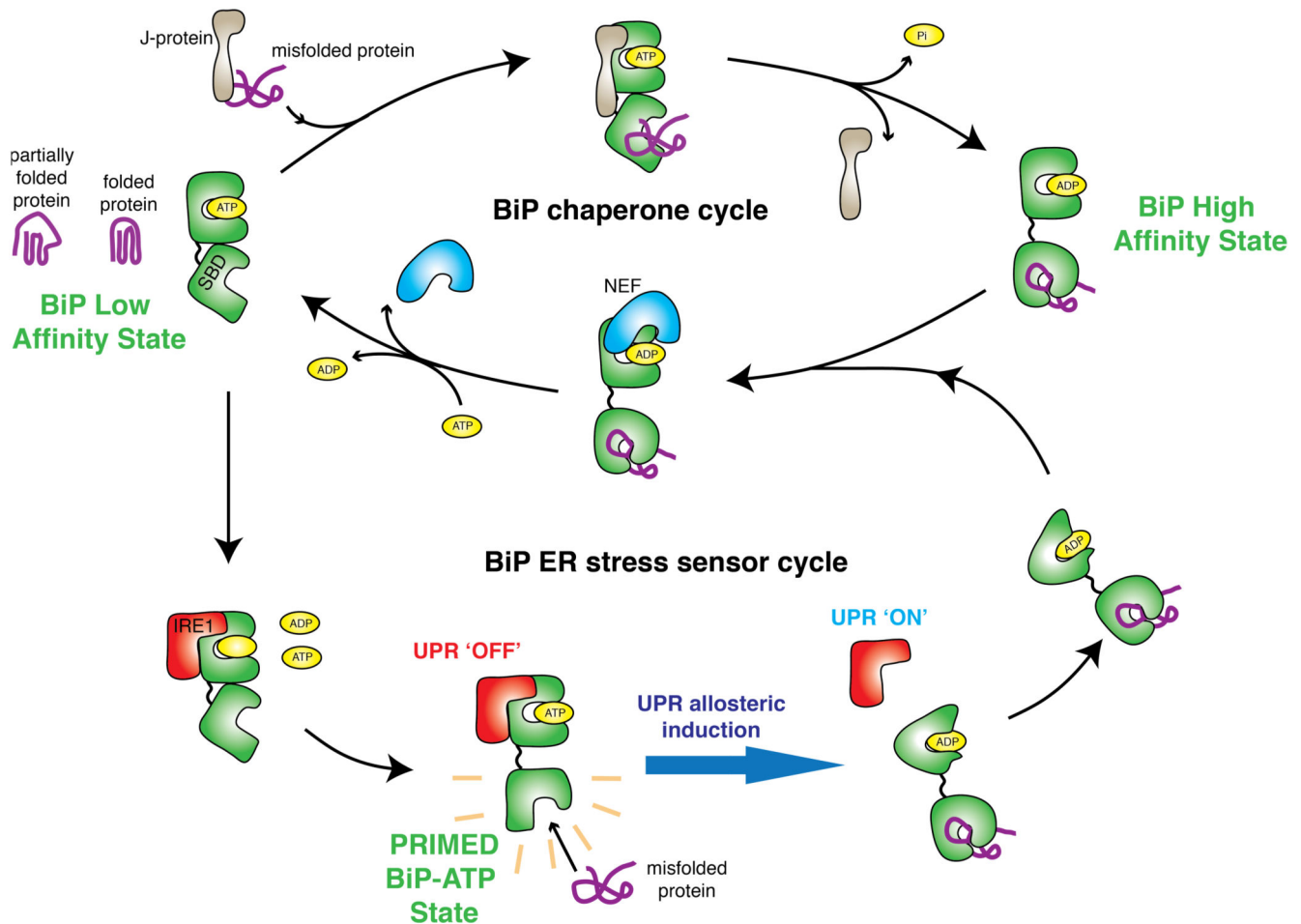
Figure 6. Mechanism of BiP function encompassing its chaperone and ER stress sensor cycles.
Interaction with UPR proteins switch BiP from chaperone cycle to ER stress sensor cycle by preventing binding to cochaperone and NEF proteins, with loss of BiP ATPase stimulation. The interaction between IRE1 LD is mediated via BiP NBD, whilst dissociation of complex is dependent on misfolded protein binding to BiP SBD. The BiP-IRE1 complex in the ATP bound state, has a greater sensitivity for misfolded protein, thereby facilitating release. By contrast the complex is desensitized to misfolded protein when bound to ADP. The release of BiP from UPR proteins via conformational change[21,22] – is coupled to UPR activation[34], enabling BiP to interact with cochaperones and revert to its chaperone cycle with misfolded protein attached.